sciendo

LATVIAN JOURNAL OF PHYSICS
AND TECHNICAL SCIENCES
2023, N 3

DOI: 10.2478/lpts-2023-0018

STUDY OF THE PERFORMANCE OF A PHOTOVOLTAIC SOLAR PANEL BY USING A NANOFLUID AS A COOLER

R. Abdeldjebar[1]*, M. Elmir[1,2], M. Douha[1]

[1]Energetics in Arid Zones Laboratory,
Faculty of Technology, TAHRI Mohamed University of Bechar,
P.O.Box 417, 08000, Bechar, ALGERIA
[2]Mechanics, Modelling and Experimentation Laboratory,
Faculty of Technology, TAHRI Mohamed University of Bechar,
P.O.Box 417, 0800, Bechar, ALGERIA
* e-mail: rachid.abdeldjebar@univ-bechar.dz

In this paper, we study by numerical simulation, the cooling of a solar photovoltaic panel using a nanofluid as a cooler. The solar panel is subjected to a hot temperature that characterises the climate of the city of Bechar located in southwestern Algeria. The nanofluid (Al2O3-water) is introduced in the cavity with a constant horizontal speed and subjected to the ambient (cold) temperature. The equations governing the hydrodynamics of the flow and the heat transfer are described by the Navier-Stockes and energy equations. The finite element method is used to solve the system of partial differential equations (PDEs) based on the Galerkin method. We consider the effect of solid volume fraction and form factor for different values of Reynolds number on the results in the form of isotherms, streamlines, temperature, velocity, average Nusselt numbers and solar panel efficiency.

Keywords: *Finite element method, forced convection, nanofluid, photovoltaic solar panel.*

1. INTRODUCTION

Global warming, rising fuel oil prices and other environmental factors in today's world are prompting energy sector organisations to develop green energy technologies for use in commercial and residential markets. One of these technologies was invented in 1894 by regions with a hot climate such as the region of Bechar located in the southwest of Algeria.

The surface temperatures of photovol-

taic panels increase due to the low yield of solar energy in electricity, because not all the energy absorbed by the photovoltaic cells can be converted into electrical energy. To satisfy the law of conservation of energy, the remaining solar energy must be converted into heat. The efficiency of photovoltaic cells is further reduced when installed in environments with hot climates, as the heat dissipation of the panels is reduced. Therefore, it is relevant to develop PV cell cooling methods to increase the output efficiency. The research [2] found that poorly ventilated PV panels in high ambient temperature environments could reach temperatures above 90 °C. These conditions are not only dangerous, but also reduce the efficiency and life of the panels. To date, active and passive methods of cooling photovoltaic panels have been studied and analysed. The authors in [3] studied an active cooling system for PV panels, in which the PV panels were cooled by forced convection, air being the coolant. This system allowed an increase in electrical efficiency of 4 to 5%.

Researchers [4] studied cooling combined photovoltaic-thermal solar panel by using water. This was accomplished by numerically solving the EDP system by the finite element method. The increase in the electrical efficiency of the panel at different operating temperatures was calculated from the thermal coefficient of the PV cells. The paper [5] presents the effect of nanofluids as a coolant in a solar photovoltaic panel. The authors have studied the effect of temperature on solar panels installed in the region of India where the temperature can reach 50 °C. The latter directly influences the conversion efficiency of solar energy into electricity. For this reason, they used fluids and nanofluids to cool solar cells. Rubbi et al. [6] reported results that indicated the overall efficacy of the MXene soybean oil-based nanoscale fluids compared to conventional fluids used for the purpose of cooling in the PV/T. Morphological studies carried out by Scanning electron microscopy showed spherical shape nanoparticles of CuO and leaf-shaped Al2O3 in particles with submicron range. In [7], the researchers studied the importance in the choice of coolant materials with base fluids for solar panel applications by plotting I-V and P-V spectrum. As a result, the cooling efficiency of both CuO and Al_2O_3 were found to be 18.2 %, which was higher than the conventional one. The obtained efficiency value was also compared with the reported data. This shows that CuO and Al_2O_3 will be a promising candidate with a base fluid of water for solar panel applications.

Abdallah et al. [8] presented a new experimental study on the use of hydrogel beads with different bed configurations as a cooling accessory under the solar panel. The best results were obtained using three rows of hydrogel beads with fins where the panel temperature dropped approximately 10 °C below the uncooled panel at 1000W/m leading to an increase in electricity production efficiency of 7.2 % compared to the uncooled system. The research [9] examined the increase in performance of the PV panel. The combination of PCM (OM35) and water as a cooling medium was experimentally evaluated. It was determined that the integrated PCM water cooling technology with continuous water supply contributed to the efficient thermal management of the PV panel which, in turn, improved the power output performance compared to cooling with the maximum permissible temperature mechanism.

Moreover, performance parameters such as electrical efficiency, electricity generation, power boost ratio, average temperature reduction, total power output and

total energy efficiency are evaluated and reported as the water requirements of the building that can be allowed to pass through the PCM. The research [10] tests the effect of different designs for indoor and outdoor systems and the effect of using salt water in cooling solar panels. It is believed to be among the first experiments to study the use of salt water as a way to remove heat from solar panels in order to reduce the temperature of the PV module. It can be concluded that: Compared with the non-cooled panels, the new proposed internal configuration reduced the panel temperature by (12 °C and 14 °C) at the intensity of 800 W/m2 and 1000 W/m2 of solar radiation. The results showed that salt water can be used as an alternative to pure water because it gives the same performance. Although having the same performance, it is preferable to use salt water due to its availability and high potential for using this system for desalination purposes (future work).

Activated alumina tablets showed a higher spoilage rate at higher salinity. Kabeel and Abdelgaied [11] used quenching to reduce the surface temperature of the PV. On the other hand, inverters were used to reduce reflection loss and increase the rate of solar radiation absorbed by photovoltaic panels, several operating cases were studied. The cooling air coming out of the PV module was injected for two cases into the upgraded solar module to increase the rate of evaporation inside the solar collector, thus improving the freshwater productivity. The use of the air injection system also improved the fresh water production compared to the case without the air injection system. The average overall efficiency of the hybrid system was recorded. Peng et al. [12] studied the effect of solar PV surface temperature on the output performance, in particular, the efficiency was studied. Experimental work was carried out under various irradiation conditions to explore the variance of output voltage, current, output power and efficiency. Next, a cooling test was performed to see how much efficiency improvement could be achieved with the cooling condition. Since the test results showed that solar PV efficiency could have an increased rate of 47% with cooling condition, a cooling system was proposed to prepare a potential system for residential solar PV application. Sahay et al. [13] tested panel cooling system, using smoke flow visualization technology. There was a marked increase in the conversion efficiency due to the cooling of the PV panels. The data were analysed using ANOVA analysis to determine the causal effect of the cooling action. The cooling system was modified. If combined with the solar PV panel design, the cooling was expected to be more effective and thus better conversion efficiency was achieved. Singh et al. [14] developed new hybrid designs for converged collector ducts to a divergent chimney combined with an inlet bell orifice design that improved flow velocity by 71% and reduced the temperature of the PV panel by 8–12 ° C. The increased flow velocity boosted turbine power output by over 200 %. Certainly, the new hybrid solar chimney design added a contribution to the research community in developing a high-efficiency solar chimney design in order to meet future energy requirements. This study reinforces work previously done [4], by using identical PV/T plate and thermal glue properties. However, the study used a thin rectangular tank through which water flew and carried heat away from the panel. It is a cooling tank attached to the back of the panel by an approximate thermal paste of uniform thickness of 0.3 mm over the entire surface area of the tank PV panel user interface. The walls of the tank are approximately 1 mm thick and made of aluminium. Aluminium was chosen as

the tank container material, due to its high thermal conductivity that promotes heat transfer across its boundaries, availability, and relatively low cost compared to other conductive metals such as copper.

The objective of this study is to increase the performance of a solar photovoltaic panel installed in an arid region such as the city of Bechar located in south-western Algeria. To achieve this objective, nanofluid is used to cool the solar panel. The configuration used in this study is shown in Fig. 1.

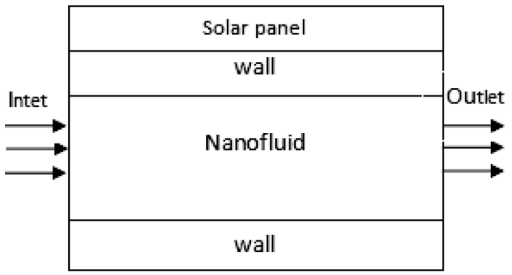


Fig. 1. Physical model

2. MATHEMATICAL FORMULATION

The flow of the nanofluid in the cooling line and the heat transfer between the panel and the nanofluid are governed by the conservation of mass, momentum and energy equations.

To solve the system of partial differential equations (PDEs), we adopt the following simplifying assumptions:

- The physical properties of the nanofluid are constant.
- The flow is laminar and bidimensional.

Using a Cartesian coordinate system and taking into account simplifying assumptions, the system of equations takes the following form:

In nanofluid zone

- Continuity equation:

$$\frac{\partial u}{\partial x}+\frac{\partial v}{\partial y}=0 \tag{1}$$

- Equation of momentum following x:

$$u\frac{\partial u}{\partial x}+v\frac{\partial u}{\partial y}=-\frac{1}{\rho_{nf}}\frac{\partial p}{\partial x}+\frac{\mu_{nf}}{\rho_{nf}}\left(\frac{\partial^2 u}{\partial^2 x}+\frac{\partial^2 u}{\partial^2 y}\right) \tag{2}$$

- Equation of momentum following y:

$$u\frac{\partial v}{\partial x}+v\frac{\partial v}{\partial y}=-\frac{1}{\rho_{nf}}\frac{\partial p}{\partial y}+\frac{\mu_{nf}}{\rho_{nf}}\left(\frac{\partial^2 v}{\partial^2 x}+\frac{\partial^2 v}{\partial^2 y}\right) \tag{3}$$

Energy equation:

$$u\frac{\partial T}{\partial x}+v\frac{\partial T}{\partial y}=\alpha_{nf}\left(\frac{\partial^2 T}{\partial^2 x}+\frac{\partial^2 T}{\partial^2 y}\right) \tag{4}$$

In solid zones

$$\frac{\partial^2 T}{\partial^2 x}+\frac{\partial^2 T}{\partial^2 y}=0 \tag{5}$$

With: $\alpha_{nf}=\dfrac{k_{nf}}{(\rho c_p)_{nf}}$

$$\rho_{nf}=(1-\phi)\rho_f+\phi\rho_s \tag{6}$$

$$\mu_{nf}=\frac{\mu_f}{(1-\phi)^{2.5}} \tag{7}$$

$$k_{nf}=k_f\frac{(2-2\phi)k_f+(1+\phi)k_s}{(2+\phi)k_f+(1-\phi)k_s} \tag{8}$$

$$(\rho c_p)_{nf}=(1-\phi)(\rho c_p)+\phi(\rho c_p)_s \tag{9}$$

Dimensionless equations:

Equations (1) to (5) can be converted to the dimensionless forms by using the following parameters:

$$X = \frac{x}{D},\ Y = \frac{y}{D},\ U = \frac{u}{U_0},\ V = \frac{v}{U_0},$$

$$P = \frac{p}{\rho_{nf} {U_0}^2},\ \theta = \frac{T - T_c}{T_h - T_c}.$$

Therefore, using the above parameters leads to dimensionless forms of the governing equations as below:

In nanofluid zone

$$\frac{\partial U}{\partial X} + \frac{\partial V}{\partial Y} = 0 \tag{10}$$

$$U\frac{\partial U}{\partial X} + V\frac{\partial U}{\partial Y} = \frac{\partial p}{\partial X} + \frac{1}{\left((1-\phi+\phi R_\rho)(1-\phi)^{2.5}\right)} \frac{1}{\mathrm{Re}}\left(\frac{\partial^2 U}{\partial X^2} + \frac{\partial^2 U}{\partial Y^2}\right) \tag{11}$$

$$U\frac{\partial V}{\partial X} + V\frac{\partial V}{\partial Y} = \frac{\partial p}{\partial y} + \frac{1}{\left((1-\phi+\phi R_\rho)(1-\phi)^{2.5}\right)} \frac{1}{\mathrm{Re}}\left(\frac{\partial^2 V}{\partial X^2} + \frac{\partial^2 V}{\partial Y^2}\right) \tag{12}$$

$$U\frac{\partial \theta}{\partial X} + V\frac{\partial \theta}{\partial Y} = \frac{1}{1-\phi+\phi R_{(\rho C_p)}} \frac{2-2\phi+(1+\phi)R_K}{2+\phi+(1-\phi)R_K} \frac{1}{\mathrm{Pr}\ \mathrm{Re}}\left(\frac{\partial^2 \theta}{\partial^2 X} + \frac{\partial^2 \theta}{\partial^2 Y}\right) \tag{13}$$

In solid zones

$$\left(\frac{\partial^2 \theta}{\partial^2 X} + \frac{\partial^2 \theta}{\partial^2 Y}\right) = 0 \tag{14}$$

Where:

$$Pr = \frac{\mu_f}{\rho_f \alpha_f},\ Re = \frac{UD\rho_f}{\mu_f},\ R_\rho = \frac{\rho_s}{\rho_f},$$

$$R_k = \frac{k_s}{k_f},\ R_{(\rho C_P)} = \frac{(\rho c_p)_s}{(\rho c_p)_f}.$$

The table below includes the boundary conditions used to solve the above system of equations

Inlet	U=1; V=0; θ=0
Outlet	P=0; Convective flux
Nanofluid-wall interface	U=V=0; Continuity
Wall-solar panel interface	U=V=0; Continuity
Top wall	U=V=0; T=1
Bottom wall	U=V=0, Adiabatic

3. RESULTS AND DISCUSSION

The finite element method is used in our model for discretizing the governing equations ((10) to (13)) along with the boundary conditions. We tested several meshes and opted for a mesh composed of 40000 elements. To describe the structure of the flow in the cavity, we fixed the following parameters of the nanofluid (Al2O3-water):

$$Pr=7,\ R_\rho=3.885,\ R_k=60,\ R_{(\rho Cp)}=0.718.$$

3.1 Streamlines and Isotherms

Figures 2 to 7 show the streamlines (left) and isotherms (right) for a form factor (A=15.25 and A=61), for different values of the Reynolds number (5≤Re ≤50) and varying the nanoparticles volume concentration from 0 % to 10 %. Regardless of the value of Re and φ, the streamlines are in the form of horizontal lines parallel to each other. The intensity of the flow is most intense at the axis of symmetry of the pipe. According to the shape of the isotherms, and by fixing the volume fraction, we notice that the energy dissipation decreases with the increase of the Reynolds number Re, which means that in order to dissipate more heat from the solar collector, low velocities are

used at the inlet of the pipe. The addition of the nanoparticles decreases the flow intensity, thus promoting an increase in the heat dissipation of the collector in the nanofluid.

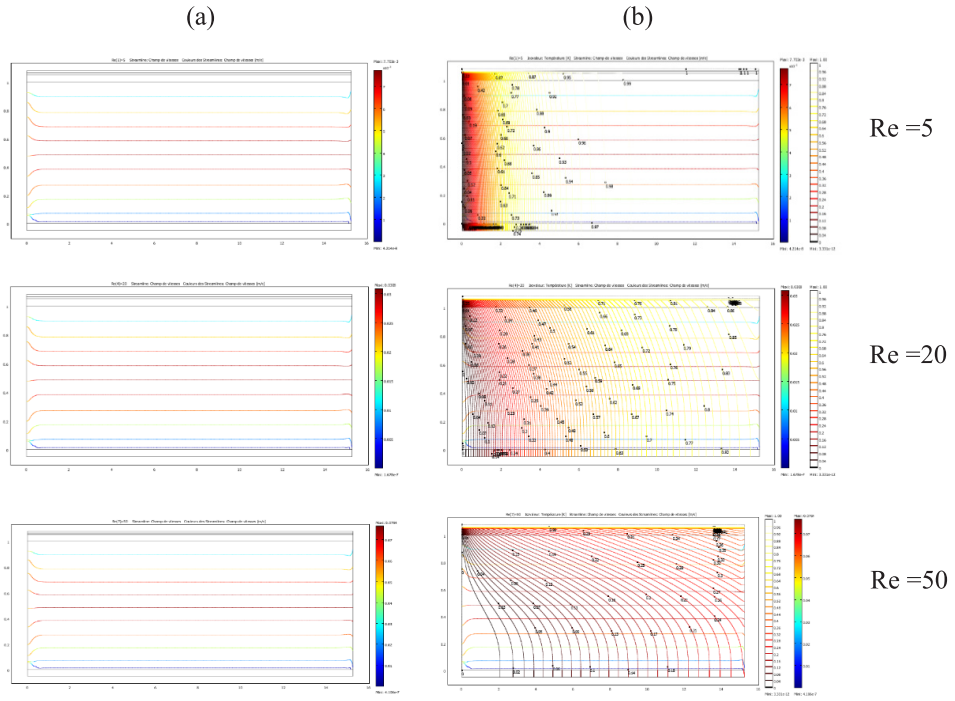


Fig. 2. Streamlines (a) and isotherms (b) for A=15.25 and φ=0.00.

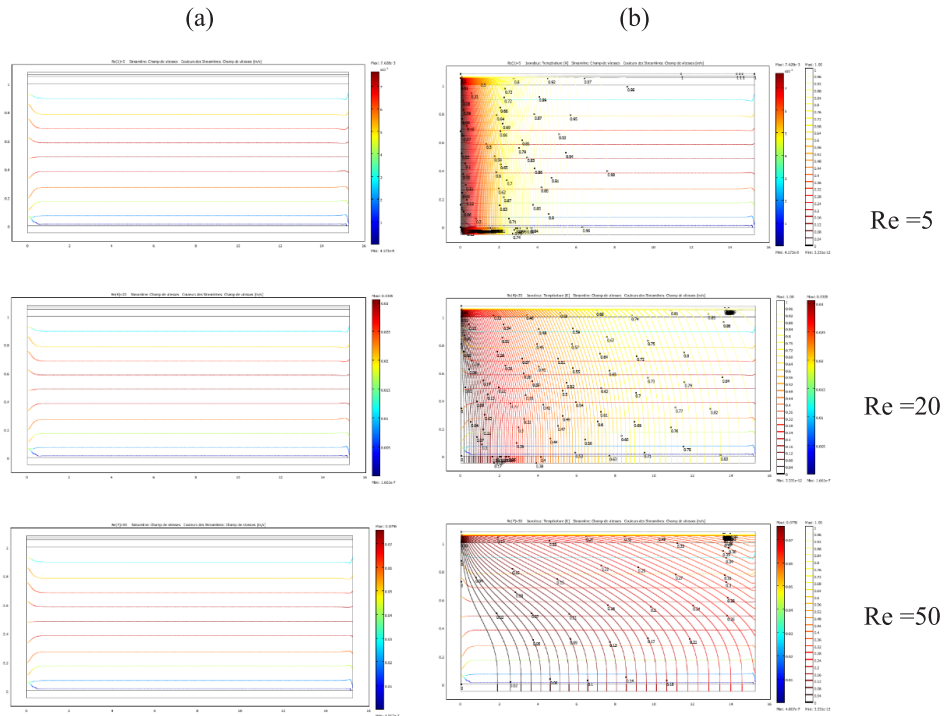


Fig. 3. Streamlines (a) and isotherms (b) for A=15.25 and φ=0.05.

(a) (b)

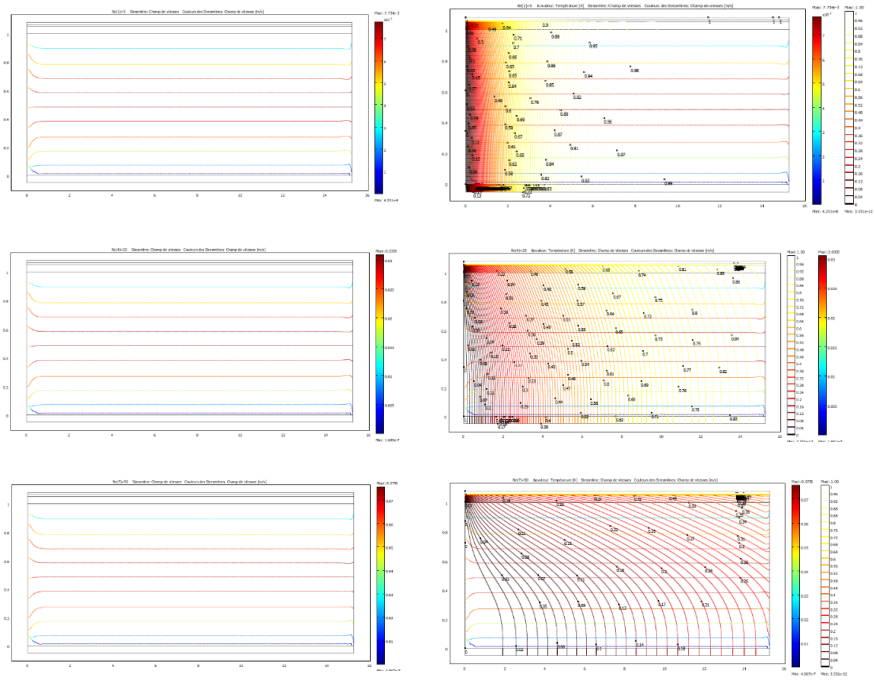


Fig. 4. Streamlines (a) and isotherms (b) for A=15.25 and φ=0.10.

(a) (b)

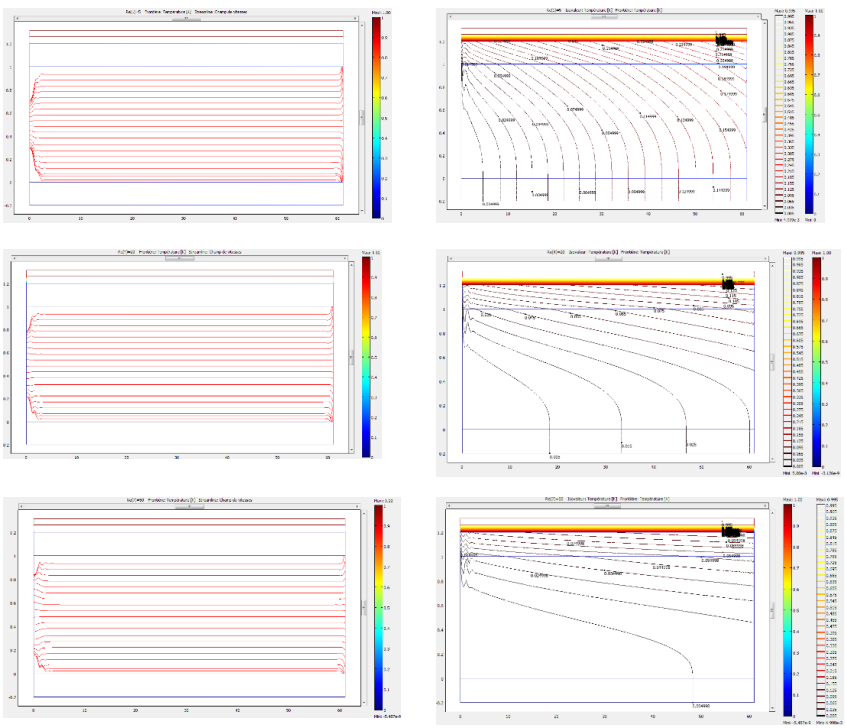


Fig. 5. Streamlines (a) and isotherms (b) for A=61 and φ=0.00.

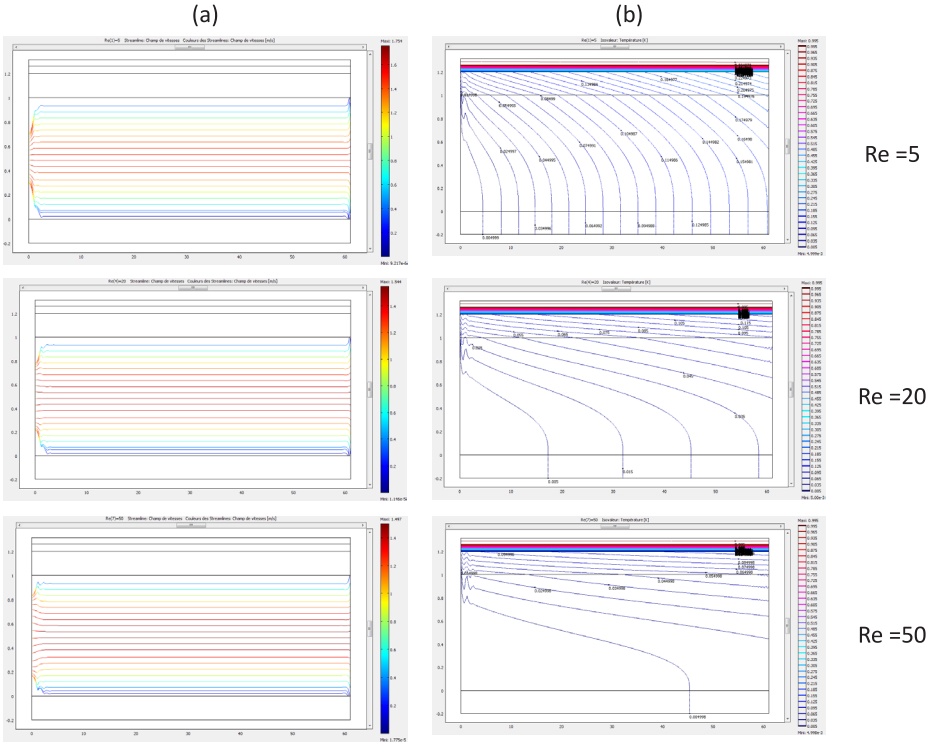


Fig. 6. Streamlines (a) and isotherms (b) for A=61 and j=0.05.

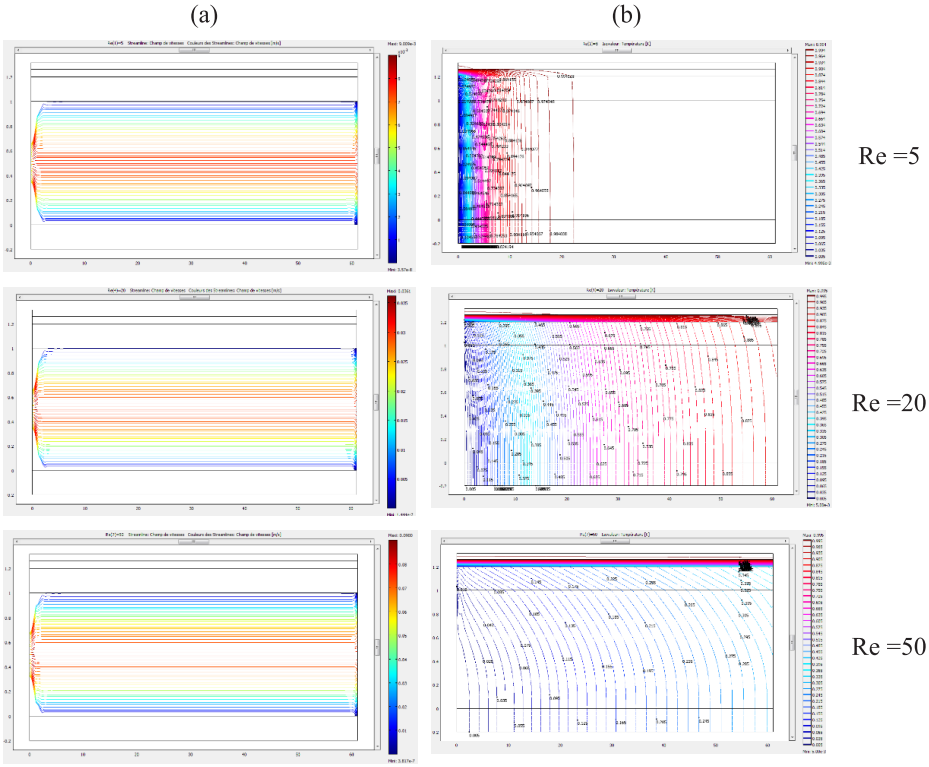


Fig. 7. Streamlines (a) and isotherms (b) for A=61 and φ=0.10.

3.2. Maximum Stream Function

Figure 8 shows the evolution of the maximum current function as a function of the form factor for different values of the volume fraction and Reynolds number.

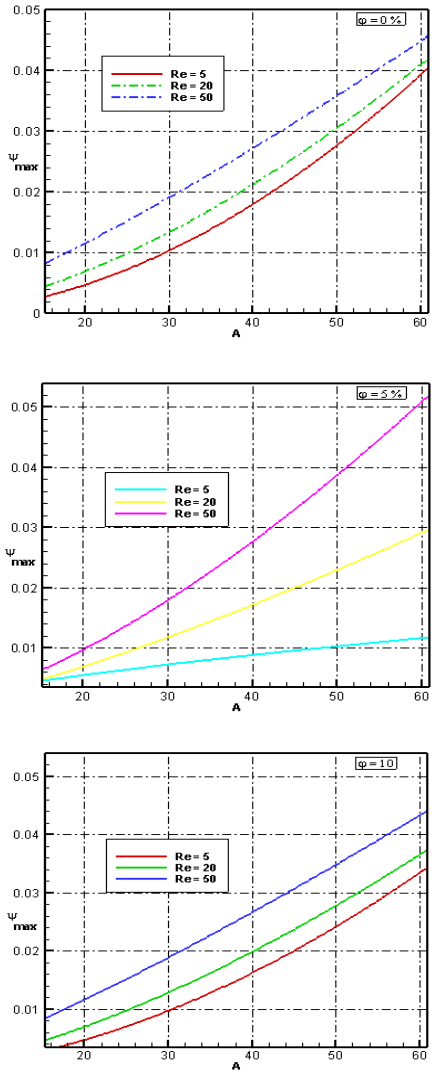


Fig. 8. Stream function vs aspect ratio.

By fixing the value of the form factor (A), the value of the maximum current function increases with increasing Reynolds number.

For a constant volume fraction and whatever the value of the Re number, the maximum current function increases with the increase of the form factor. By fixing the geometrical characteristics of the configuration and for a constant flow rate of the nanofluid, the maximum current function decreases with the increase of the nanoparticles volume fraction.

3.3. Average Velocity

Figure 9 represents the evolution of the average speed U_{avg} as a function of the Reynolds number Re for different values of the form factor A and ϕ varying between 0 % and 10 %.

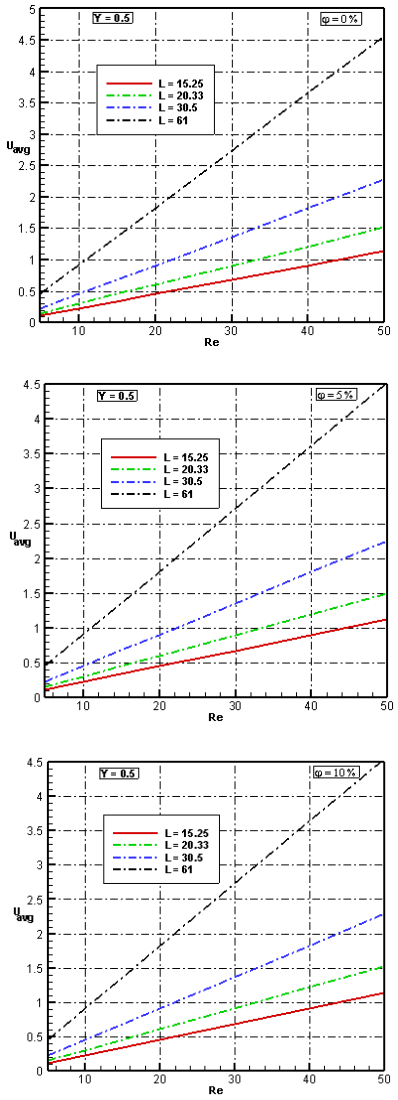


Fig. 9. Average velocity vs Re.

Whatever the value of the aspect ratio A, the flow is more intense at the lower wall of the sensor.

For A = 15.25 and A = 20.33, the intensity is large in the middle of this wall and this intensity shifts to the left for other values of A.

Whatever the value of A and φ the change in the average speed as a function of Re is linear:

$$U_{avr} = a\,\mathrm{Re} + b$$

A		15.25	20.33	30.50	61.00
φ=0.00	a	0.0227	0.0206	0.0455	0.0914
	b	0.0002	0.0927	0.0001	0.0004
φ=0.05	a	0.0225	0.0300	0.0451	0.0905
	b	0.0002	0.0002	0.0001	0.0004
φ=0.10	a	0.0228	0.0304	0.0457	0.0910
	b	0.0002	0.0002	0.0001	0.004

3.4. Temperature Evolution

The curve of Figure 10 represents the evolution of the temperature along the vertical passing through the middle of the pipe for Re = 5 and for different values of φ and A. The temperature increases as it approaches the lower wall of the sensor until a maximum value is reached. This maximum value decreases with the increase of A.

Figure 11 represents the evolution of the temperature along the horizontal passing through the middle of the pipe for Re = 5, A=15.25 and for different values of φ. The temperature increases as it approaches the lower wall of the sensor until a maximum value is reached.

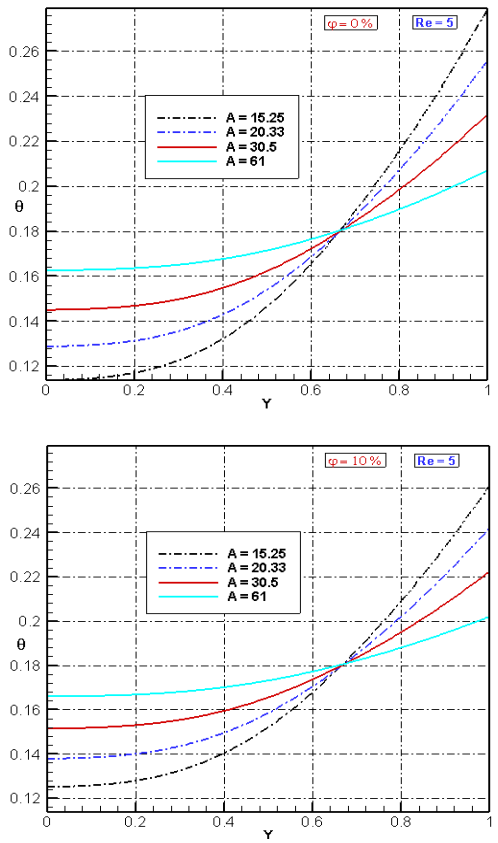


Fig. 10. Temperature evolution vs Y.

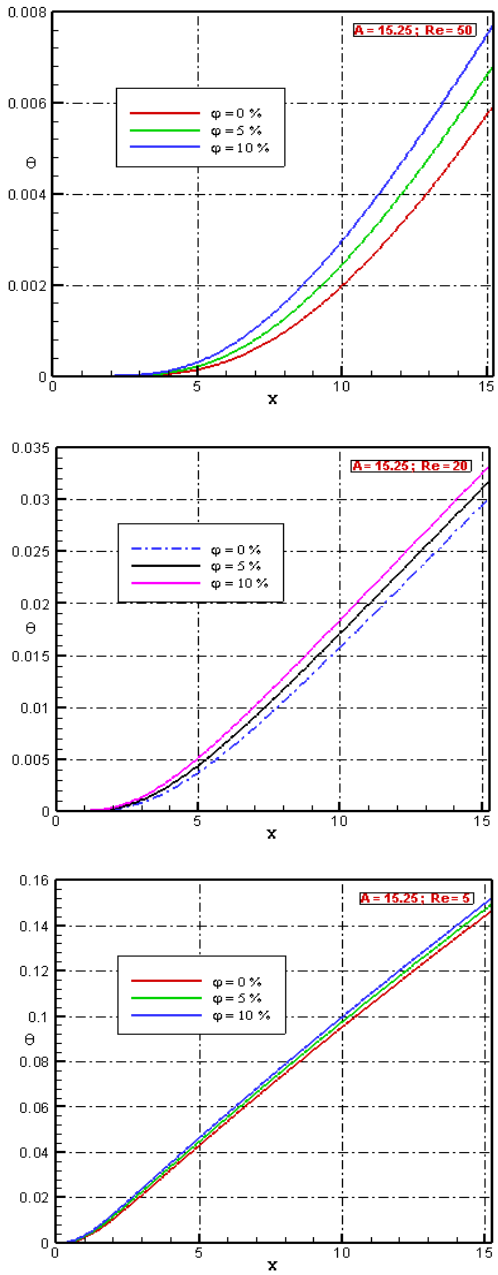


Fig. 11. Temperature evolution vs X.

3.5. Average Nusselt Number

Figure 12 demonstrates the evolution of average Nusselt number with Reynolds number for different values of aspect ratio ($15.25 \leq A \leq 61$) and for the base fluid ($\varphi = 0$) and two values of volume concentration.

For a given volume fraction, the Nusselt number increases with increasing form factor and decreases with increasing Nusselt. The cooling is done for a low inlet velocity.

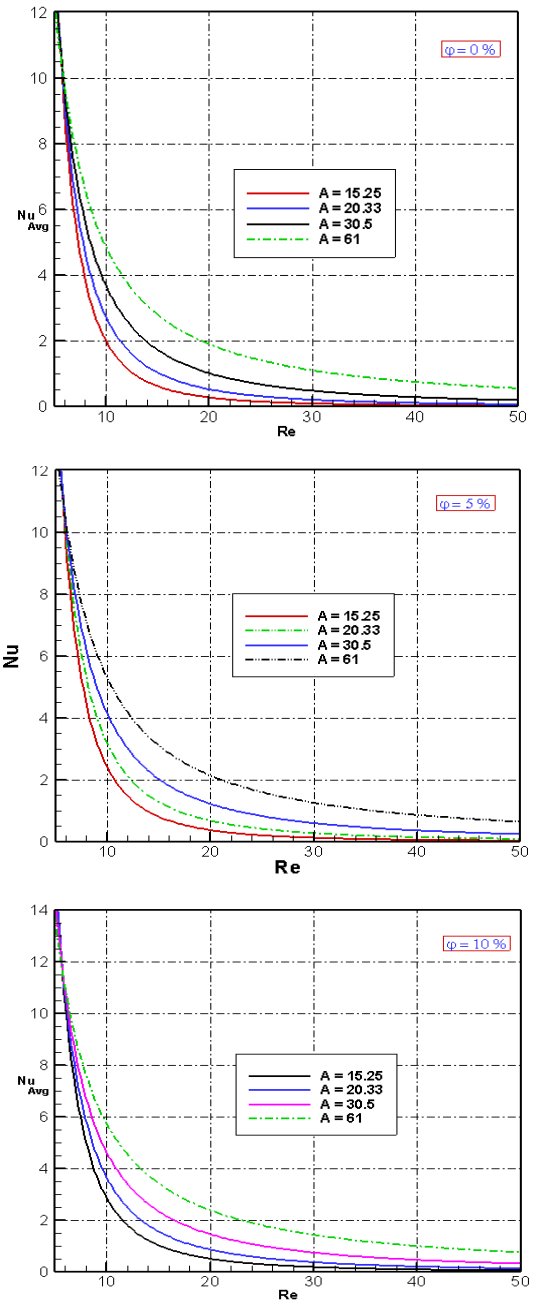


Fig. 12. Average Nusselt vs Re.

3.6. Cell Efficiency

Figure 13 shows the change in the efficiency of the solar cell as a function of Re for three values of volume fraction (ϕ=0; ϕ=0.05 and ϕ=0.10). Whatever the value of A, the efficiency (η) decreases with the increase of Re, the optimal configuration corresponds to A = 30.50.

Whatever the value of the form factor (A), the flow is more intense at the level of the lower wall of the collector. For A = 15.25

and A = 20 the intensity is large in the middle of this wall; this intensity shifts to the left for the other values of A.

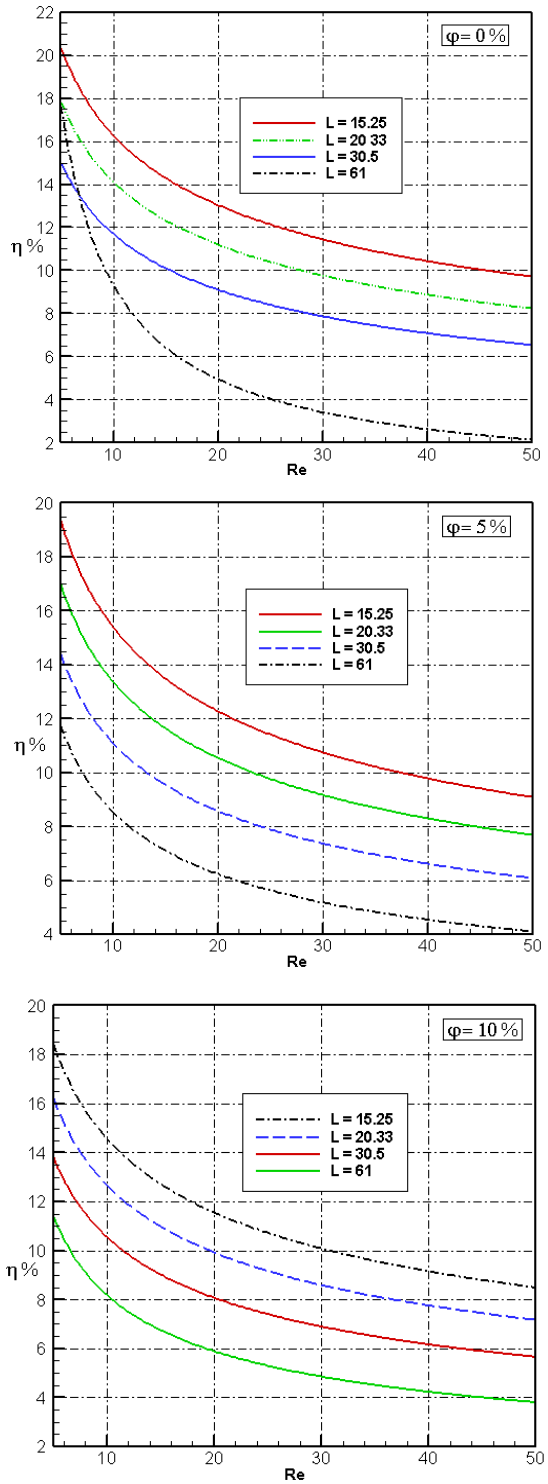


Fig. 13. Cell efficiency evolution.

4. CONCLUSIONS

Solar photovoltaic (PV) panels under extreme weather conditions considerably reduce their operation efficiency. It is envisaged to cool the solar panels by using a nanofluid as a cooler. The main results of this study are as follows:

- the addition of nanoparticles increases the heat exchange rate between the panel and the nanofluid when compared with the base fluid;
- low flow rate increases the exchange rate, which provides good cooling;
- longer pipes increase the efficiency of the solar panel.

ACKNOWLEDGEMENTS

We gratefully acknowledge the General Directorate of Scientific Research and Technological Development (DGRSDT) for its financial support and unwavering encouragement.

REFERENCES

1. Nelson, J. (2003). *The Physics of Solar Cells*. London: Imperial College Press.
2. Oh, J., & TamizhMani, G. (2010). Temperature testing and analysis of PV modules per ANSI/UL 1703 and IEC 61730 standards. In *35th IEEE Photovoltaic Specialists Conference*, (pp. 984–988), 20–25 June 2010. Honolulu, HI, USA.
3. Teo, H.G., Lee, P.S., & Hawlader, M.N.A. (2012). An Active Cooling System for Photovoltaic Modules. *Applied Energy, 90*, 309–315.
4. Fontenault, B. J., & Gutierrez-Miravete, E. (2012). Modeling Combined Photovoltaic-Thermal Solar Panel. *Proceedings of the 2012 COMSOL Conference in Boston*. Available at https://www.comsol.com/paper/download/150907/gutierrezmiravete_presentation.pdf
5. Suresh, A.K., Khurana, S., Nandan, G., Dwivedi, G., & Kumar, S. (2018). Role on Nanofluids in Cooling Solar Photovoltaic Cell to Enhance Overall Efficiency. *Materials Today: Proceedings, 5,* 20614–20620.
6. Rubbi, F., Habib, K., Saidur, R., Aslfattahi, N., Yahya, S.M., & Das, L. (2020). Performance Optimization of a Hybrid PV/T Solar System Using Soybean Oil/MXene Nanofluids as a New Class of Heat Transfer Fluids. *Solar Energy, 208*, 124 –138.
7. Amalraj, S., & Michael, P.A. (2019). Synthesis and Characterization of Al_2O_3 and CuO Nanoparticles into Nanofluids for Solar Panel Applications. *Result in Physics 2019*, *15*, 102797.
8. Abdallah, S. R., Saidani-Scott, H., Benedi, J., & Abdelrahman, M. A. (2020). Hydrogels Beads for Cooling Solar Panels: Experimental Study. *Renewable Energy, 153*, 777–786.
9. Sudhakar, P., Santosh, R., Asthalakshmi, B., Kumaresan, G., & Velraj, R. (2020). Performance Augmentation of Solar Photovoltaic Panel through PCM Integrated Natural Water Circulation Cooling Technique. *Renewable Energy, Elsevier, 172 (C*), 1433–1448.
10. Abdo, S., Saidani-Scott, H., Borges, B., & Abdelrahman, M.A. (2020). Cooling Solar Panels Using Saturated Activated Alumina with Saline Water: Experimental Study. *Solar Energy, 208*, 345–356.

11. Kabeel, A. E., Abdelgaied, M. (2019). Performance Enhancement of a Photovoltaic Panel with Reflectors and Cooling Coupled to a Solar Still with Air Injection. *Journal of Cleaner Production, 224*, 40–49.
12. Peng, Z., Herfatmanesh, M.R., & Liu, Y. (2017). Cooled Solar PV Panels for Output Energy Efficiency Optimization. *Energy Conversion and Management*, *150*, 949–955.
13. Sahay, A., Sethi, V.K., Tiwari, A., & Pandey, M. (2015). A Review of Solar Photovoltaic Panel Cooling Systems with Special Reference to Ground Coupled Central Panel Cooling System (GC-CPCS). *Renewable and Sustainable Energy Reviews, 42* (C), 306–312.
14. Singh, A.P., Kumar, A., Singh, O.P., & Akshayveer. (2020). Strategies for Effective Cooling of Photovoltaic Panels Integrated with Solar Chimney. *Materials Today: Proceedings, 39 (5),* 1950–1954.